PROCEEDINGS OF SCIENCE

Inclusive and diffractive dijet photoproduction in UPCs at the LHC in NLO QCD

Vadim Guzey*
National Research Center "Kurchatov Institute", Petersburg Nuclear Physics Institute (PNPI), Gatchina, 188300, Russia
Department of Physics, University of Jyväskylä, P.O. Box 35, 40014 University of Jyväskylä, Finland
Helsinki Institute of Physics, P.O. Box 64, 00014 University of Helsinki, Finland
E-mail: guzey_va@nrcki.pnpi.ru

Michael Klasen†‡
Institut für Theoretische Physik, Westfälische Wilhelms-Universität Münster, Wilhelm-Klemm-Straße 9, 48149 Münster, Germany
E-mail: michael.klasen@uni-muenster.de

We present a next-to-leading order QCD calculation of inclusive dijet photoproduction in ultra-peripheral Pb-Pb collisions at the LHC and show that the results agree very well with various kinematic distributions measured by the ATLAS collaboration. The effect of including these data in nCTEQ or EPPS16 nuclear parton density functions (nPDFs) is then studied using the Bayesian reweighting technique. For an assumed total error of 5% on the final data, its inclusion would lead to a significant reduction of the nPDF uncertainties of up to a factor of two at small values of the parton momentum fraction. As an outlook, we discuss future analyes of diffractive nPDFs, which are so far completely unknown.

European Physical Society Conference on High Energy Physics - EPS-HEP2019 -
10-17 July, 2019
Ghent, Belgium

*Work supported by RFBR through the grant 17-52-12070.
†Speaker.
‡Work supported by the DFG through the grant KL 1266/9-1.

PoS(EPS-HEP2019)302

1. Motivation

Ultraperipheral collisions (UPCs) of relativistic ions are defined by a large impact parameter b that exceeds the sum of the nuclear radii R_A. At these large distances, short-range strong nuclear forces are suppressed. The nuclei interact instead electromagnetically through long-range photon exchanges in $\gamma\gamma$ and γA reactions, in particular when they are as heavily charged as lead ions ($Z = 82$) [1]. Interesting examples of physics processes in UPCs include quarkonium and dilepton pair production, light-by-light scattering and searches for physics beyond the Standard Model. Here we focus on inclusive dijet photoproduction in Pb-Pb collisions at the LHC, which has recently been observed and analysed by the ATLAS collaboration [2].

Apart from the novelty of the observation, this process is particularly interesting for future constraints on nuclear parton distribution functions (PDFs) $f_{j/A}(x,Q^2)$ [3, 4]. They can be modeled from their bare proton counterparts $f_{j/p}(x,Q^2)$ with a multiplicative factor $R_j^A(x,Q^2)$, which captures the nuclear modifications. Depending on the region in the momentum fraction x, different effects have been observed. At low x, the shadowing suppression can be interpreted as the absorption by surface nucleons of the virtual photon probing the nucleus after fluctuating into $q\bar{q}$ dipoles. Shadowing is compensated at intermediate x by antishadowing as imposed by the momentum sum rule. At large x, nuclear PDFs are again reduced by the EMC effect, interpreted in various ways like valence quark suppression due to nuclear binding, pion exchange, quark clusters, short-range correlations, etc. At very large x, Fermi motion of the nucleons leads to nuclear enhancement. The extraction of nuclear PDFs suffers from large uncertainties, in particular for gluons at small x, so that the inclusion of LHC and future EIC data is very important [5, 6] .

2. Inclusive dijet photoproduction at the LHC

A potentially interesting novel process in this respect is inclusive dijet photoproduction in UPCs at the LHC, which has recently been observed and analysed by the ATLAS collaboration [2]. We have computed this process in NLO QCD [7], based on previous work on inclusive jet [8] and dijet [9], real and virtual [10] photoproduction in ep collisions at HERA (for a review see [11]). As shown in Fig. 1, direct (left) and resolved (right) photons contribute to these processes.

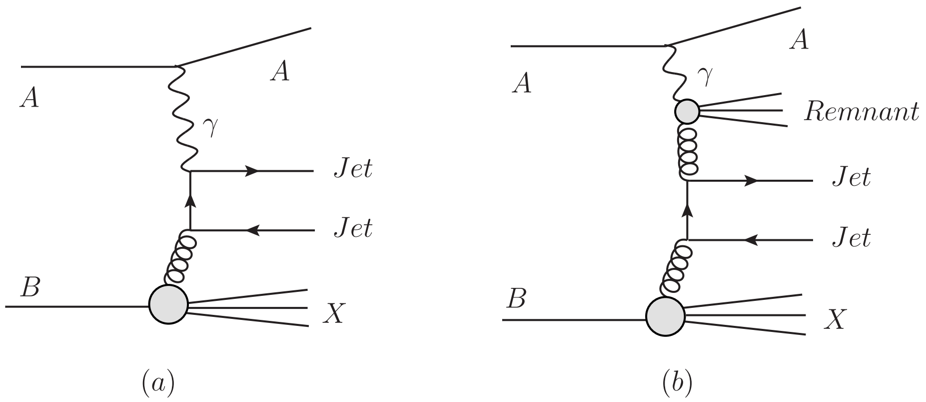

Figure 1: Direct (left) and resolved (right) photoproduction of dijets in ultraperipheral collisions of nuclei A and B at the LHC.

The differential hadronic cross sections

$$d\sigma(AB \to AB + 2\text{jets} + X) = \sum_{a,b} \int dy \int dx_\gamma \int dx_A\, f_{\gamma/A}(y) f_{a/\gamma}(x_\gamma, \mu_f^2) f_{b/B}(x_A, \mu_f^2) d\hat{\sigma}(ab \to \text{jets}) \tag{2.1}$$

are related to those of partons a and b, $d\hat{\sigma}(ab \to \text{jets})$, by the photon flux $f_{\gamma/A}(y)$ and PDFs $f_{a/\gamma}(x_\gamma, \mu_f^2)$, where the former are well described by

$$f_{\gamma/A}(y) = \frac{2\alpha Z^2}{\pi}\frac{1}{y}\left[\zeta K_0(\zeta)K_1(\zeta) - \frac{\zeta^2}{2}(K_1^2(\zeta) - K_0^2(\zeta))\right] \tag{2.2}$$

for a relativistic pointlike charge Z with $\zeta = y m_p b_{\min}$, assuming no strong interactions for $b > b_{\min} = 2.1 R_{\text{Pb}} = 14.2\,\text{fm}$. The latter are taken from the GRV NLO parameterisation [12], while we adopt nCTEQ15 nuclear PDFs [3] and estimate their uncertainty by summing over independent eigenvectors, $\Delta\sigma = \frac{1}{2}\sqrt{\sum_{k=1}^{31}(\sigma(f_k) - \sigma(f_{k+1}))^2}$. The renormalisation and factorisation scales are set to $\mu_r = \mu_f = 2E_{T,1}$, where the points of fastest convergence of the perturbative seires and of minimal scale sensitivity coincide. Jets are defined with the anti-k_T algorithm and distance parameter $R = 0.4$, transverse energies $E_{T,1} > 20$ GeV, $E_{T,2} > 15$ GeV, $H_T = \sum_i E_{T,i} > 35$ GeV, rapidities $|\eta_{1,2}| < 4.4$ and a combined jet mass $m_{\text{jets}} > 35$ GeV.

The comparison of our calculations with the - unfortunately still preliminary - ATLAS data [2] is shown in Fig. 2. On a logartihmic scale, we find excellent agreement not only in the total transverse energy (H_T, left) and parton momentum fraction distributions in the lead ion (x_A, right), but also for the parton momentum fraction distributions in the photon (z_γ, not shown). Note, however, that the data have not yet been unfolded for detector response.

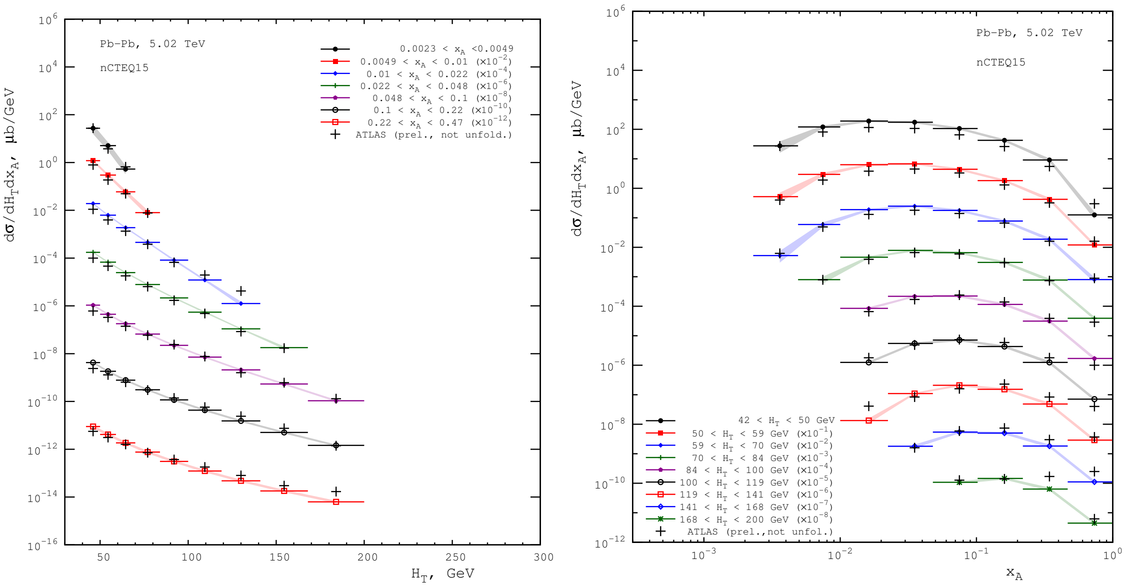

Figure 2: Inclusive dijet photoproduction at the LHC as measured by ATLAS, compared to our NLO QCD calculations. Shown are the double-differential total transverse energy (left) and parton momentum fraction distributions in the target lead ion (right) [7].

PoS(EPS-HEP2019)302

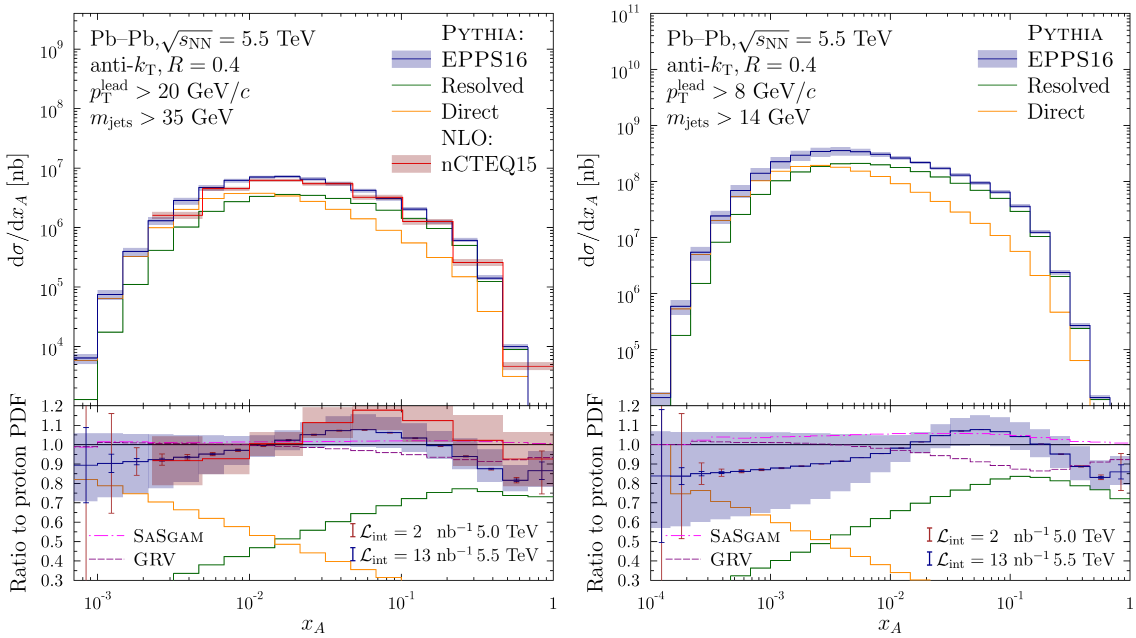

Figure 3: Single-differential parton momentum fraction distributions integrated over H_T for the HL-/HE-LHC and 5.5 TeV centre-of-mass energy with original (left) and low-x_A-extended ATLAS acceptance (right) [13]. Also shown are simulations with PYTHIA 8, direct and resolved contributions separately, and the dependence on the photon PDFs [14].

For the high-luminosity (HL) and high-energy (HE) LHC community study, we have updated our predictions from 5.02 to 5.5 TeV centre-of-mass energy per nucleon [13]. The results are shown in Fig. 3. We observe a large potential for improvement in the nuclear shadowing region, in particular if the ATLAS modifies the acceptance from the current transverse energy cuts (left) to lower values (right). As one can see, the resolved photon PDF sensitivity resides mostly at large x_A corresponding to small z_γ or low E_T, while the direct process dominates at small x_A.

3. Bayesian reweighting

Using our NLO QCD calculations presented in the previous section, we went on to study the impact of dijet photoproduction data at the LHC on future determinations of nuclear PDFs [15]. Denoting the central fits of the nCTEQ15 [3] and EPPS16 [4] analyses by $f^0_{j/A}$ for parton j and nucleus A and the error sets by $f^{i\pm}_{j/A}$ ($i = 1\dots 2N$ with $N = 16$ for nCTEQ15, based on CTEQ6.1M proton PDFs, and $N = 20+28$ for nuclear + proton PDF uncertainties in EPPS16), we produced replicas $k = 1\dots N_{\rm rep}$ with $N_{\rm rep} = 10,000$ through

$$f^k_{j/A}(x,Q^2) = f^0_{j/A}(x,Q^2) + \frac{1}{2}\sum_{i=1}^{N}\left[f^{i+}_{j/A}(x,Q^2) - f^{i-}_{j/A}(x,Q^2)\right] R_{ki} \tag{3.1}$$

with a normally distributed random number R_{ki} ($\mu = 0, \sigma = 1$) as well as pseudodata from our NLO QCD prediction for $d\sigma^0/dx_A$ with the central PDFs $f^0_{j/A}$ for $N_{\rm data} = 9$ bins in x_A. We then

Table 1: Effective number of contributing replicas in our nPDF reweighting study.

ε	$N_{\rm eff}$(nCTEQ15)	$N_{\rm eff}$(nCTEQ15np)	$N_{\rm eff}$(EPPS16)
0.05	4407	3982	5982
0.1	7483	7742	8727
0.15	8870	9107	9555
0.2	9464	9607	9818

evaluated the test function

$$\chi_k^2 = \sum_{j=1}^{N_{\rm data}} \frac{(d\sigma^0/dx_A - d\sigma^k/dx_A)^2}{\sigma_j^2} \tag{3.2}$$

with assumed uncertainties $\sigma_j = \varepsilon d\sigma^0/dx_A$ for different assumptions on the data precision $\varepsilon = 0.05\ldots0.2$. This allowed us to obtain reweighted nPDFs

$$\langle f_{j/A}(x,Q^2)\rangle_{\rm new} = \frac{1}{N_{\rm rep}} \sum_{k=1}^{N_{\rm rep}} w_k f^k_{j/A}(x,Q^2) \tag{3.3}$$

and their uncertainties

$$\delta\langle f_{j/A}(x,Q^2)\rangle_{\rm new} = \sqrt{\frac{1}{N_{\rm rep}} \sum_{k=1}^{N_{\rm rep}} w_k \left(f^k_{j/A} - \langle f_{j/A}(x,Q^2)\rangle_{\rm new}\right)^2} \tag{3.4}$$

from the weights

$$w_k = \frac{e^{-\frac{1}{2}\chi_k^2/T}}{\frac{1}{N_{\rm rep}} \sum_i^{N_{\rm rep}} e^{-\frac{1}{2}\chi_i^2/T}}, \tag{3.5}$$

where $\sum_k w_k = N_{\rm rep}$ and the tolerances were $T = 35$ and 52 for nCTEQ15 and EPPS16, respectively. The effective numbers of contributing replicas are then

$$N_{\rm eff} = \exp\left[\frac{1}{N_{\rm rep}} \sum_k^{N_{\rm rep}} w_k \ln(N_{\rm rep}/w_k)\right]. \tag{3.6}$$

They are listed in Tab. 1. The impact of the final ATLAS data with an assumed total uncertainty of $\varepsilon = 0.05$ on the nPDFs can be deduced from Fig. 4. In this case, the uncertainty of the nCTEQ15np fit, which does not use pion data from RHIC, is reduced by about a factor of two, in particular at low x_A.

4. Diffractive dijet photoproduction

A completely novel set of PDFs, namely diffractive nuclear PDFs $f^{D(4)}_{b/A}(x_{I\!P}, z_{I\!P}, t, \mu^2)$, appears in cross sections of diffractive dijet photoproduction

$$d\sigma = \sum_{a,b} \int dt \int dx_{I\!P} \int dz_{I\!P} \int dy \int dx_\gamma f_{\gamma/A}(y) f_{a/\gamma}(x_\gamma, \mu_f^2) f^{D(4)}_{b/A}(x_{I\!P}, z_{I\!P}, t, \mu_f^2) d\hat{\sigma}^{(n)}_{ab\to{\rm jets}} \tag{4.1}$$

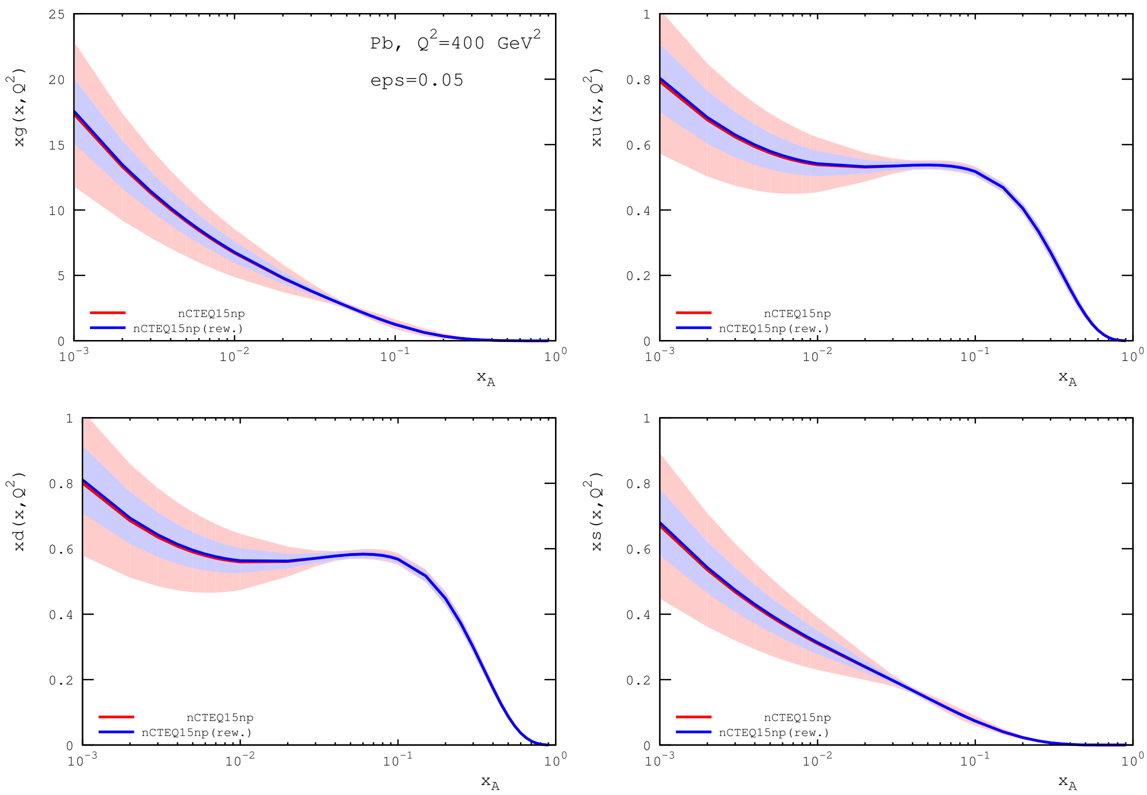

Figure 4: The gluon, u-quark, d-quark, and s-quark nCTEQ15np nPDFs as a function of x_A at $Q^2 = 400$ GeV^2 with (blue, inner band) and without (red, outer band) the Bayesian reweighting for an assumed total experimental uncertainty of $\varepsilon = 0.05$ [15].

with intact (at most excited) nuclei and/or large rapidity gaps on both sides of the event. Diffractive nuclear PDFs can be theoretically defined as conditional leading-twist distributions of partons b in nuclei A in terms of the light-cone momentum fraction $z_{I\!P}$ at the resolution scale μ_f, provided that the nucleus undergoes diffractive scattering characterised by the light-cone momentum fraction loss $x_{I\!P}$ and the invariant momentum transfer squared t. The leading-twist model of nuclear shadowing [16], which is based on a generalisation of Gribov-Glauber theory, QCD factorisation theorems and information on diffractive processes at HERA [17, 18], predicts a significant suppression of nuclear diffractive PDFs

$$f_{b/A}^{D(4)}(x_{I\!P}, z_{I\!P}, t, \mu_f^2) = R_b(x_{I\!P}, z_{I\!P}, \mu_f^2) f_{b/A}^{D(4),\mathrm{IA}}(x_{I\!P}, z_{I\!P}, t, \mu_f^2) \tag{4.2}$$

at low $x_A = x_{I\!P} z_{I\!P}$ compared to the impulse approximation (IA). Note that Eq. (4.2) breaks in principle the phenomenological factorisation of diffractive PDFs into the product of a Pomeron ($I\!P$) flux and Pomeron PDFs. However, the shadowing suppression $R_b(x_{I\!P}, z_{I\!P}, \mu^2)$ depends only weakly on the parton flavor b, the scale μ_f, $z_{I\!P}$ and $x_{I\!P}$ and can in practice be approximated by a factor of 0.15.

In a recent study, we have made predictions in NLO QCD for diffractive dijet photoproduction in pp, p-Pb and Pb-Pb collisions at the LHC [19]. Distributions for the latter at a center-of-mass energy per nucleon of $\sqrt{s_{NN}} = 2.76$ TeV are shown in Fig. 5. Approximate results for p-Pb and pp collisions and can be obtained by a simple rescaling with A based on the approximate re-

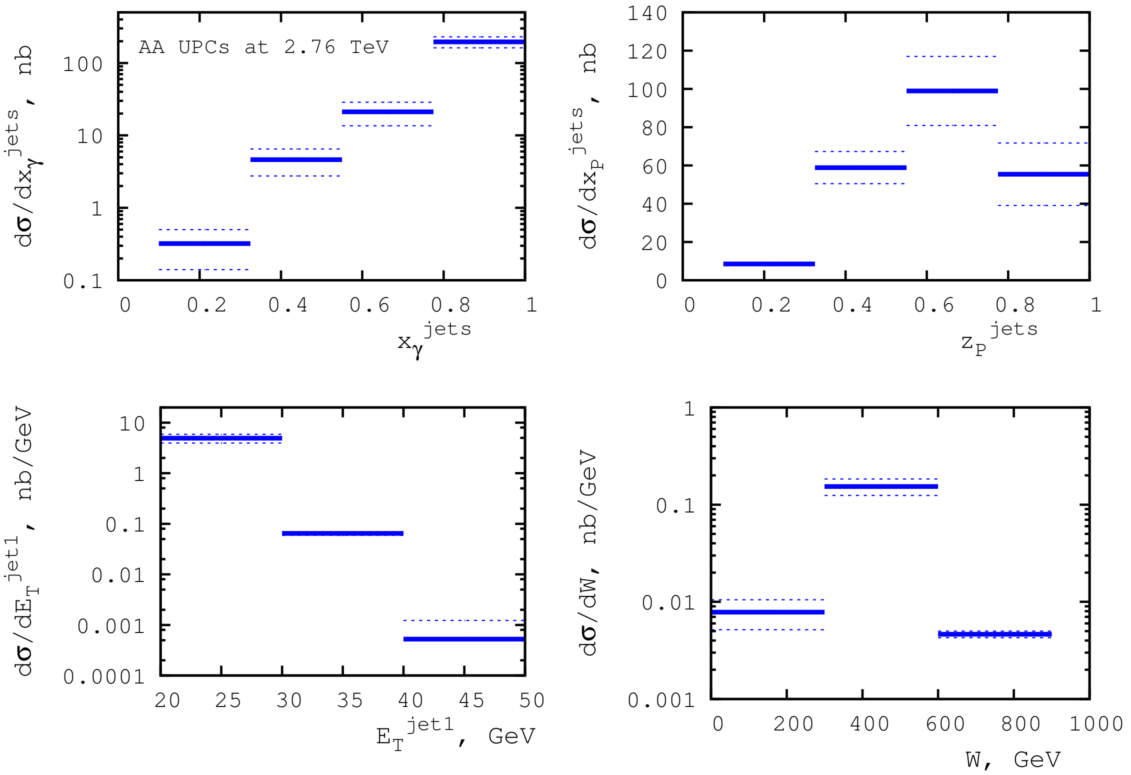

Figure 5: Differential cross sections for diffractive photoproduction of dijets $d\sigma(AA \to A + 2\text{jets} + X' + A)$ in Pb-Pb UPCs at $\sqrt{s_{NN}} = 2.76$ TeV.

lation $f^{D(3)}_{b/A}(x_{I\!P}, z_{I\!P}, \mu_f^2) \approx A/2 f^{D(3)}_{b/p}(x_{I\!P}, z_{I\!P}, \mu_f^2)$ between the nuclear and proton diffractive PDFs (integrated over the momentum transfer t) and the fact that the Pb-Pb cross section receives contributions of both nuclei, while the p-Pb cross section is dominated by the photon-from-nucleus contribution.

It is well known from studies of diffractive photoproduction of dijets in ep scattering at HERA that collinear factorisation for this process is broken, *i.e.* NLO QCD calculations overestimate the measured cross sections by almost a factor of two. The pattern of this factorization breaking remains unknown and presents one of the outstanding questions in this field [17, 18], but it would in principle of course also apply to diffractive dijet photoproduction in UPCs at the LHC [19].

5. Conclusion

In conclusion, we have presented an NLO QCD analysis of dijet photoproduction in UPCs at the LHC, where short-range strong interactions are suppressed. On a logarithmic scale, our calculations agreed very well with preliminary ATLAS data, which unfortunately must still be unfolded for detector effects. In a Bayesian reweighting study, we showed that the final data have the potential to reduce the uncertainties of nuclear PDFs, in particular in the shadowing region at small parton momentum fractions, by about a factor of two. If the nuclei on both sides of the interaction stay intact or have large rapidity gaps to the central hard event, an interesting novel quantity, namely diffractive nuclear PDFs can be extracted, in particular, but not only, from diffractive dijet photoproduction, and QCD factorisation breaking in these processes can be analysed in detail.

References

[1] A. J. Baltz *et al.*, Phys. Rept. **458** (2008) 1.

[2] The ATLAS collaboration [ATLAS Collaboration], ATLAS-CONF-2017-011.

[3] K. Kovarik *et al.*, Phys. Rev. D **93** (2016) 085037; K. Kovarik, P. M. Nadolsky and D. E. Soper, arXiv:1905.06957 [hep-ph]; D. B. Clark *et al.* [nCTEQ Collaboration], arXiv:1909.00452 [hep-ph].

[4] K. J. Eskola, P. Paakkinen, H. Paukkunen and C. A. Salgado, Eur. Phys. J. C **77** (2017) 163.

[5] E. C. Aschenauer, S. Fazio, M. A. C. Lamont, H. Paukkunen and P. Zurita, Phys. Rev. D **96** (2017) 114005.

[6] M. Klasen, K. Kovarik and J. Potthoff, Phys. Rev. D **95** (2017) 094013; M. Klasen and K. Kovarik, Phys. Rev. D **97** (2018) 114013.

[7] V. Guzey and M. Klasen, Phys. Rev. C **99** (2019) 065202.

[8] M. Klasen, G. Kramer and S. G. Salesch, Z. Phys. C **68** (1995) 113; M. Klasen, G. Kramer and M. Michael, Phys. Rev. D **89** (2014) 074032.

[9] M. Klasen and G. Kramer, Phys. Lett. B **366** (1996) 385; Z. Phys. C **72** (1996) 107; Z. Phys. C **76** (1997) 67; Eur. Phys. J. C **71** (2011) 1774; M. Klasen, T. Kleinwort and G. Kramer, Eur. Phys. J. direct **1** (1998) 1.

[10] M. Klasen, G. Kramer and B. Pötter, Eur. Phys. J. C **1** (1998) 261; T. Biekötter, M. Klasen and G. Kramer, Phys. Rev. D **92** (2015) 074037.

[11] M. Klasen, Rev. Mod. Phys. **74** (2002) 1221.

[12] M. Glück, E. Reya and A. Vogt, Phys. Rev. D **46** (1992) 1973.

[13] Z. Citron *et al.*, arXiv:1812.06772 [hep-ph].

[14] I. Helenius, PoS DIS **2018** (2018) 113.

[15] V. Guzey and M. Klasen, Eur. Phys. J. C **79** (2019) 396.

[16] L. Frankfurt, V. Guzey and M. Strikman, Phys. Rept. **512** (2012) 255.

[17] M. Klasen and G. Kramer, Eur. Phys. J. C **38** (2004) 93; Phys. Rev. Lett. **93** (2004) 232002; J. Phys. G **31** (2005) 1391; Mod. Phys. Lett. A **23** (2008) 1885; Eur. Phys. J. C **70** (2010) 91; Phys. Lett. B **508** (2001) 259; Eur. Phys. J. C **49** (2007) 957; Phys. Rev. D **80** (2009) 074006;

[18] V. Guzey and M. Klasen, Eur. Phys. J. C **76** (2016) 467.

[19] V. Guzey and M. Klasen, JHEP **1604** (2016) 158.

PoS(EPS-HEP2019)302